Evaluation of Endogenous Metabolic Markers of Hepatic CYP3A Activity Using Metabolic Profiling and Midazolam Clearance

K-H Shin[1], MH Choi[2], KS Lim[1], K-S Yu[1], I-J Jang[1] and J-Y Cho[1]

This study aimed to evaluate endogenous metabolic markers of hepatic cytochrome P450 (CYP)3A activity in healthy subjects using a metabolomics approach. Twenty-four subjects received the following medication during the following three study periods: 1 mg of i.v. midazolam alone (control phase), 1 mg of i.v. midazolam after 4 days of pretreatment with 400 mg of ketoconazole once daily (CYP3A-inhibited phase), and 2.5 mg of i.v. midazolam after 10 days of pretreatment with 600 mg of rifampicin once daily (CYP3A-induced phase). During each study period, 24 h before and after the administration of midazolam, urine samples were collected at 12-h intervals for metabolomic analyses. We derived an equation to predict midazolam clearance (CL) based on several of these markers. We demonstrated that a combination of the concentrations and ratios of several endogenous metabolites and the *CYP3A5*3* genotype is a reliable predictive marker of hepatic CYP3A activity as assessed by i.v. administration of midazolam.

Cytochrome P450 (CYP)3A is involved in the oxidative metabolism of a wide range of endogenous metabolites and exogenous compounds.[1] More than 50% of therapeutic drugs are metabolized by CYP3A;[2] therefore, the possibility of drug–drug interactions mediated by the inhibition and induction of CYP3A is critically important for the development of new therapeutics. CYP3A metabolism exhibits a high level of interindividual variation, which may result from the expression of the CYP3A4 and CYP3A5 isoforms and their regulation by endogenous metabolites or coadministered drugs. The dominant CYP isoform, CYP3A4, which is highly expressed in the liver and intestine, has several genetic variants, including *CYP3A4*18* and *CYP3A4*22*, that can alter the protein levels or metabolic function of CYP3A.[3–6] CYP3A5 is expressed in most Africans but in few Caucasians and Asians. The wild-type, functional *CYP3A5*1* allele is present in 14% of Swedes, 33% of Koreans, and 74% of Tanzanians.[7–9] The expression of CYP3A enzymes is regulated by nuclear receptors, including the pregnane X receptor (NR1I2), the vitamin D receptor, and retinoid X receptor α, and different levels of regulation can cause high interindividual variation in CYP3A activity.[10–12] Therefore, phenotyping CYP3A activity is important for determining individual CYP3A metabolic activity and for characterizing the inhibitory or inducible features of a new drug.

Several endogenous markers of CYP3A activity have been reported, including the urinary level of 6β-hydroxycortisol, the urinary ratio of 6β-hydroxycortisol:cortisol, and the plasma level of 4β-hydroxycholesterol.[9,13,14] 4β-hydroxycholesterol is an endogenous CYP3A marker that is related to the *CYP3A5* genotype, and its plasma concentration correlates well with CYP3A activity.[14] However, due to its long half-life (more than 60 h)[15] and low sensitivity,[16] 4β-hydroxycholesterol might not be a good marker for predicting the basal level or inhibition of CYP3A activity. The urinary 6β-hydroxycortisol:cortisol ratio has been used as an endogenous marker of CYP3A4 induction by rifampicin, but this marker was not found to be a reliable measure of actual CYP3A4 activity.[17] Recently, the sum of the clearance (CL) of 6β-hydroxycortisol and 6β-hydroxycortisone was found to be a more useful indicator of CYP3A4 inhibition *in vivo* as compared with the CL of either 6β-hydroxycortisol or 6β-hydroxycortisone alone.[18] However, the efficacy of this sum for measuring CYP3A4 induction *in vivo* has not been evaluated. Therefore, new approaches are needed to identify endogenous biomarkers of both the induction and the inhibition of CYP3A *in vivo*.

Metabolomics is an approach that allows for the simultaneous survey of all the low-molecular-weight molecules and metabolites present in bodily fluids.[19] Because metabolites are sensitive to biological changes resulting from disease, genetic alterations, or environmental changes,[20] a combination of the levels of metabolites (a metabolic signature) can be used as a

[1]Department of Clinical Pharmacology and Therapeutics, Seoul National University College of Medicine and Hospital, Seoul, Korea; [2]Future Convergence Research Division, Korean Institute of Science and Technology, Seoul, Korea. Correspondence: J-Y Cho (joocho@snu.ac.kr)

Received 23 January 2013; accepted 10 June 2013; advance online publication 7 August 2013. doi:10.1038/clpt.2013.128

more reliable biomarker of the cellular responses to biological changes. A recent study reported that four urinary metabolites could predict systemic exposure to tacrolimus, which has a narrow therapeutic range and high interindividual variation.[21]

In the current study, gas chromatography–mass spectrometry (MS) was used to profile 47 steroids, including plasma 4β-hydroxycholesterol and urinary 6β-hydroxycortisol and 6β-hydroxycortisone, in plasma and urine samples obtained from healthy male volunteers who had been administered midazolam. By correlating the levels or ratios of metabolic markers, alone or in combination, with the CL of midazolam, we identified the markers that were associated with the induction or inhibition of CYP3A by midazolam. In addition, genetic polymorphisms were evaluated to assess their effects on the markers of CYP3A activity. Ultimately, we identified accurate and reliable biomarker combinations; using them, we generated an equation to predict midazolam CL related to the induction and inhibition of CYP3A.

RESULTS

Subjects

Twenty-six healthy male subjects were enrolled, but two subjects subsequently withdrew their informed consent. Therefore, 24 subjects between 20 and 38 years of age (mean ± SD: 26.5 ± 4.6 years) weighing 56.8–87.3 kg (69.2 ± 7.7 kg) completed the study. Safety profiles were completed for all 26 subjects, and pharmacokinetic (PK) and metabolomic analyses were performed for the 24 subjects who completed the study. There were no serious or unpredictable adverse events.

Genotyping results

The *CYP3A5*3* (A6956G), *CYP3A4*18* (T878C), and *NR1I2* (C-25385T) genotypes of the 24 subjects were evaluated. The minor allele frequencies of *CYP3A5*3*, *CYP3A4*18*, and *NR1I2* were 0.792, 0.0, and 0.292, respectively.

PK of midazolam in the CYP3A-inhibited and CYP3A-induced phases

To use the PK parameters of midazolam as the gold standard for predicting CYP3A activity, we performed PK analyses to determine the plasma concentrations of midazolam and its metabolites, 1′-hydroxymidazolam and 4-hydroxymidazolam, during the CYP3A-inhibited and CYP3A-induced experimental phases (**Table 1**).

When ketoconazole was administered before midazolam (CYP3A-inhibited phase), the midazolam exposure increased; the geometric mean ratio of the dose-normalized area under the plasma concentration–time curve extrapolated to infinity (AUC_{inf}) (90% confidence interval) of midazolam was 2.89 (2.57–3.25) as compared with the control phase, and the CL decreased from 30.08 (9.04) to 10.26 (2.59) l/h. Pretreatment with rifampicin decreased the midazolam exposure; the geometric mean ratio of the dose-normalized AUC_{inf} (90% confidence interval) of midazolam was 0.46 (0.41–0.51) as compared with the control phase (**Table 1**), and the CL increased from 30.08 (9.04) to 64.16 (12.44) l/h. The mean metabolic ratios of both 1′-hydroxymidazolam:midazolam and 4-hydroxymidazolam:midazolam were reduced in the CYP3A-inhibited phase and were increased in the CYP3A-induced phase. The dose-normalized AUC_{inf} did not differ between the *CYP3A5* genotype groups during any of the three study periods, with the exception of *CYP3A5*3/*3*, which exhibited a lower CL as compared with *CYP3A5*1/*3* in the CYP3A-induced phase ($P < 0.05$) (**Supplementary Table S1** online).

Metabolic profiling

Endogenous metabolites from the predose urine and plasma samples collected at 12-h intervals in each treatment period were measured. The fold changes as compared with the control phase are listed in **Supplementary Tables S2** and **S3** online. All of the steroids measured were significantly reduced in the CYP3A-inhibited phase as compared with the control phase. In the CYP3A-induced phase, several metabolites were increased, others were reduced, and others remained unchanged as compared with the control phase. The largest increases were observed in the urinary levels of 6β-hydroxycortisol, 6β-hydroxycortisone, and 16α-hydroxydehydroepiandrosterone (16α-hydroxy-DHEA), with 4.22-, 3.92-, and 2.20-fold increases, respectively. Among the plasma metabolites, 4β-hydroxycholesterol demonstrated the greatest increase (2.43-fold) in the CYP3A-induced phase.

Because the metabolite ratios (metabolite:parent) reflect the enzymatic activity in the metabolic pathway as compared with the concentration of each metabolite, we analyzed the metabolite ratios to identify changes in enzymatic activity (**Tables 2–3**). The changes in the urinary ratios of 16α-hydroxy-DHEA:DHEA, 7β-hydroxy-DHEA:DHEA, 6β-hydroxycortisol:cortisol,

Table 1 Pharmacokinetic parameters after a single intravenous administration of midazolam alone or concomitant dose with steady-state ketoconazole or rifampicin (*n* = 24)

Parameter	Midazolam alone	Midazolam + ketoconazole	Midazolam + rifampicin
AUC_{inf}/dose (μg·h/l/mg)	36.21 ± 11.47	102.54 ± 22.48	16.15 ± 3.08
	—	2.89 (2.57–3.25)[a]	0.46 (0.41–0.51)[a]
CL (l/h)	30.08 ± 9.04	10.26 ± 2.59	64.16 ± 12.44
	—	0.35 (0.32 – 0.37)[a]	2.19 (1.99–2.40)[a]
$t_{1/2}$ (h)	3.92 ± 1.40	9.61 ± 2.98	2.69 ± 0.70
	—	2.48 (2.10–2.93)[a]	0.70 (0.61–0.81)[a]
Metabolic ratio[b]	0.21 ± 0.06	0.04 ± 0.02	0.06 ± 0.03
	—	0.14 (0.13–0.16)[a]	0.27 (0.22–0.32)[a]
Metabolic ratio[c]	0.03 ± 0.005	0.02 ± 0.006	0.01 ± 0.003
	—	0.72 (0.64–0.81)[a]	0.20 (0.16–0.25)[a]

Values are presented as arithmetic mean ± SD.

AUC_{inf}, area under the plasma concentration vs. time curve extrapolated to infinity; AUC_{last}, area under the plasma concentration vs. time curve from the last measurable time; CL, clearance; $t_{1/2}$, terminal half-life.

[a]Ratio of geometric means (90% confidence interval). [b]AUC_{last} of 1′-hydroxy midazolam/AUC_{last} of midazolam. [c]AUC_{last} of 4-hydroxy midazolam/AUC_{last} of midazolam.

Table 2 Fold change of mean urinary metabolite ratios in the CYP3A inhibition phase and induction phase as compared with the control phase

Metabolite ratio	Fold change (inhibition phase)	Fold change (induction phase)
6β-Hydroxycortisol/cortisol	▼0.18	▲5.88
6β-Hydroxycortisone/cortisone	▼0.21	▲5.01
16α-Hydroxy-DHEA/DHEA	1.01	▲3.97
16α-Hydroxyandrostenedione/androstenedione	▼0.72	▲2.74
4-Hydroxyandrostenedione/androstenedione	▼0.71	▲2.10
7β-Hydroxy-DHEA/DHEA	▼0.34	▲1.88
6β-Hydroxyandrostenedione/androstenedione	1.05	▲1.39
16α-Hydroxytestosterone/testosterone	▼0.62	0.90
2-Hydroxyestrone/estrone	1.06	▲1.14
2-Hydroxyestradiol/estradiol	▼0.76	1.10
11β-Hydroxyandrosterone/androsterone	▼0.59	1.07
11β-Hydroxyetiocholanolone/etiocholanolone	▲1.24	1.00
11β-Hydroxyandrostenedione/androstenedione	▼0.72	▲1.47
11β-Hydroxytestosterone/testosterone	▼0.43	0.87

Data are presented as fold change as compared with control phase; increased with statistical significance (▲$P < 0.05$) in the inhibition state, decreased with statistical significance (▼$P < 0.0001$,▼$P < 0.05$) in the inhibition state, increased with statistical significance (▲$P < 0.0001$,▲$P < 0.05$) in the induction state, decreased with statistical significance (▼$P < 0.0001$,▼$P < 0.05$) in the inhibition state.

CYP3A, cytochrome P450 3A; DHEA, dehydroepiandrosterone.

Table 3 Fold change of mean plasma metabolite ratios in the CYP3A inhibition phase and induction phase as compared to the control phase

Metabolite ratio	Fold change (inhibition phase)	Fold change (induction phase)
4β-Hydroxycholesterol/cholesterol	1.07	▲2.40
11-Deoxycortisol/cortisol	▲1.95	▲1.14
16α-Hydroxytestosterone/testosterone	0.97	▼0.76
11β-Hydroxytestosterone/testosterone	0.92	▼0.76
6β-Hydroxycortisol/cortisol	1.04	▲1.48
6β-Hydroxyandrostenedione/androstenedione	1.14	▼0.80
24-Hydroxycholesterol/cholesterol	▲1.73	0.98
7β-Hydroxycholesterol/cholesterol	▲1.45	1.07
11β-Hydroxyandrostenedione/androstenedione	▼0.62	0.95
17α-Hydroxypregnenolone/pregnenolone	▼0.54	1.03
6β-Hydroxycortisone/cortisone	0.90	0.96
27-Hydroxycholesterol/cholesterol	▼0.47	0.97

Data are presented as fold change as compared with control phase; increased with statistical significance (▲$P < 0.0001$▲$P < 0.05$) in the inhibition state, decreased with statistical significance (▼$P < 0.0001$,▼ $P < 0.05$) in the inhibition state, increased with statistical significance (▲$P < 0.0001$,▲$P < 0.05$) in the induction state, decreased with statistical significance (▼$P < 0.05$) in the inhibition state.

CYP3A, cytochrome P450 3A.

and 6β-hydroxycortisone:cortisone and in the plasma level of 4β-hydroxycholesterol that were observed in the control, CYP3A-inhibited, and CYP3A-induced phases are presented in **Figure 1**. The utility of these metabolites as endogenous markers of CYP3A activity requires further assessment by comparing the individual midazolam CL associated with each.

Prediction of midazolam CL

A univariate analysis of the studied metabolites and metabolite ratios was used to identify the covariates associated with individual midazolam CL and to develop an equation for predicting hepatic CYP3A activity. The urinary ratios of 16α-hydroxy-DHEA:DHEA ($r^2 = 0.572$; $P < 0.001$), 7β-hydroxy-DHEA:DHEA ($r^2 = 0.407$; $P < 0.001$), 6β-hydroxycortisone:cortisone ($r^2 = 0.646$; $P < 0.001$), and 6β-hydroxycortisol:cortisol ($r^2 = 0.440$; $P < 0.001$) and the plasma level of 4β-hydroxycholesterol ($r^2 = 0.381$; $P < 0.001$) were highly correlated with midazolam CL (**Figure 2**).

To identify a more reliable CYP3A activity marker, the metabolites and metabolite ratios found to be correlated with midazolam CL were included in the midazolam CL equation. This equation was developed using multivariate linear regression models to identify the lowest Akaike's information criterion value. Using this equation, the combination of the most significant covariates was selected (**Supplementary Table S4** online). Ultimately, *CYP3A5*1/*3* genotype, DHEA level, 7β-hydroxy-DHEA:DHEA ratio, and 6β-hydroxycortisone:cortisone ratio were selected as the most informative covariates. The midazolam CL predicted using this model correlated well with the observed midazolam CL (**Figure 3**). The following equation was developed:

$$\ln(\mathrm{CL}) = 2.1539 + 0.2724 \times I + 0.0101 \times \mathrm{DHEA} + 0.0910 \times R1 + 0.6502 \times R2,$$

where I is 1 for *CYP3A5*1/*3* and is 0 for *CYP3A5*3/*3*; $R1$ is the 7β-hydroxy-DHEA:DHEA ratio; and $R2$ is the 6β-hydroxycortisone:cortisone ratio.

The metabolite levels did not differ between the four urine collection time points (at 12-h intervals) for each study period. Therefore, the first 12-h-interval sample from each period was used for the phenotype analysis. The data for two representative metabolites, 6β-hydroxycortisol and 6β-hydroxycortisone, from each urine collection period are presented in **Supplementary Figures S1 and S2** online. No significant differences between the metabolites were found with regard to the *CYP3A5* or *NR1I2* genotypes during each treatment phase (data not shown).

DISCUSSION

We developed an integrative approach for the prediction of individual CL that reflected the hepatic CYP3A activity in both the CYP3A-inhibited and CYP3A-induced phases. We generated midazolam PK data and urinary and plasma metabolite profiles for the control, CYP3A-inhibited, and CYP3A-induced phases. Using a statistical analysis, we identified metabolites that were highly correlated with midazolam CL, and we developed an equation to predict midazolam CL that included the significant covariates of urinary metabolite levels/ratios and *CYP3A5* genotypes. This was the first study to use metabolomic profiling to

assess individual CYP3A activity during consecutive CYP3A-inhibited and CYP3A-induced phases.

Consistent with previous reports,[22,23] we found that urinary 6β-hydroxycortisol levels, 6β-hydroxycortisone:cortisone ratios, and plasma 4β-hydroxycholesterol levels reflected CYP3A activity. Midazolam CL was highly correlated with known CYP3A markers, including the urinary ratios of 6β-hydroxycortisol:cortisol (r^2 = 0.440) and 6β-hydroxycortisone:cortisone (r^2 = 0.646), as well as the plasma level of 4β-hydroxycholesterol (r^2 = 0.381). Furthermore, the correlations between midazolam CL and both the 7β-hydroxy-DHEA:DHEA ratio (r^2 = 0.407) and the

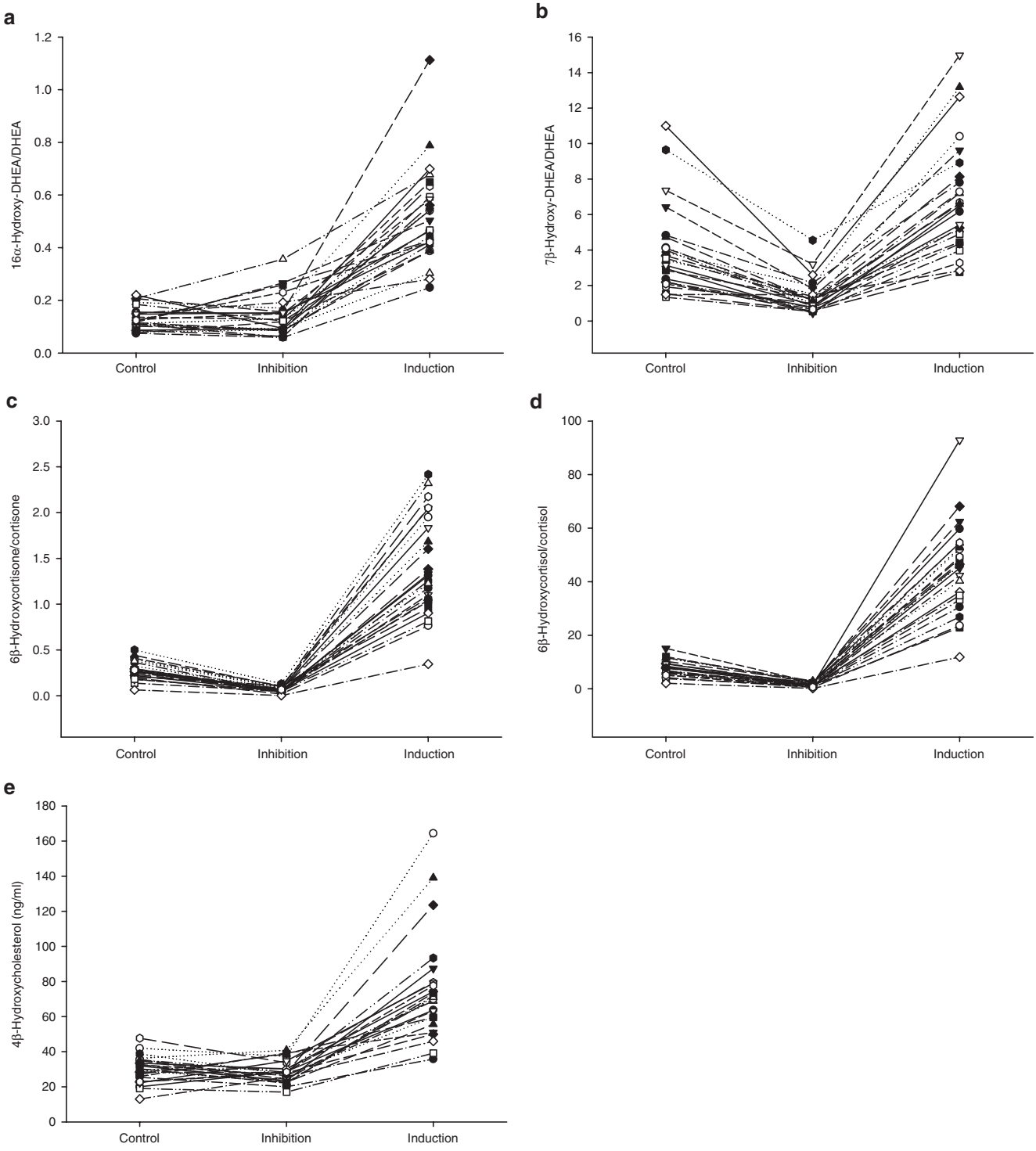


Figure 1 Individual (**a**) 16α-hydroxy-DHEA:DHEA, (**b**) 7β-hydroxy-DHEA:DHEA, (**c**) 6β-hydroxycortisone:cortisone, and (**d**) 6β-hydroxycortisol:cortisol ratios; (**e**) 4β-hydroxycholesterol levels after the administration of midazolam alone and after pretreatment with ketoconazole and rifampicin (first collection interval). DHEA, dehydroepiandrosterone.

16α-hydroxy-DHEA:DHEA ratio (r^2 = 0.572) were higher than the correlation between midazolam CL and the plasma level of 4β-hydroxycholesterol, a known CYP3A marker. Using a multivariate linear regression analysis of the significant covariates, we developed an equation to predict midazolam CL. The r^2 value (0.7046) for this equation was higher than the r^2 value for each individual covariate. Therefore, the combination of metabolite levels and ratios produced a more reliable prediction of the individual PK of CYP3A substrates in both the CYP3A-inhibited and CYP3A-induced phases. The remaining 30% could be attributed

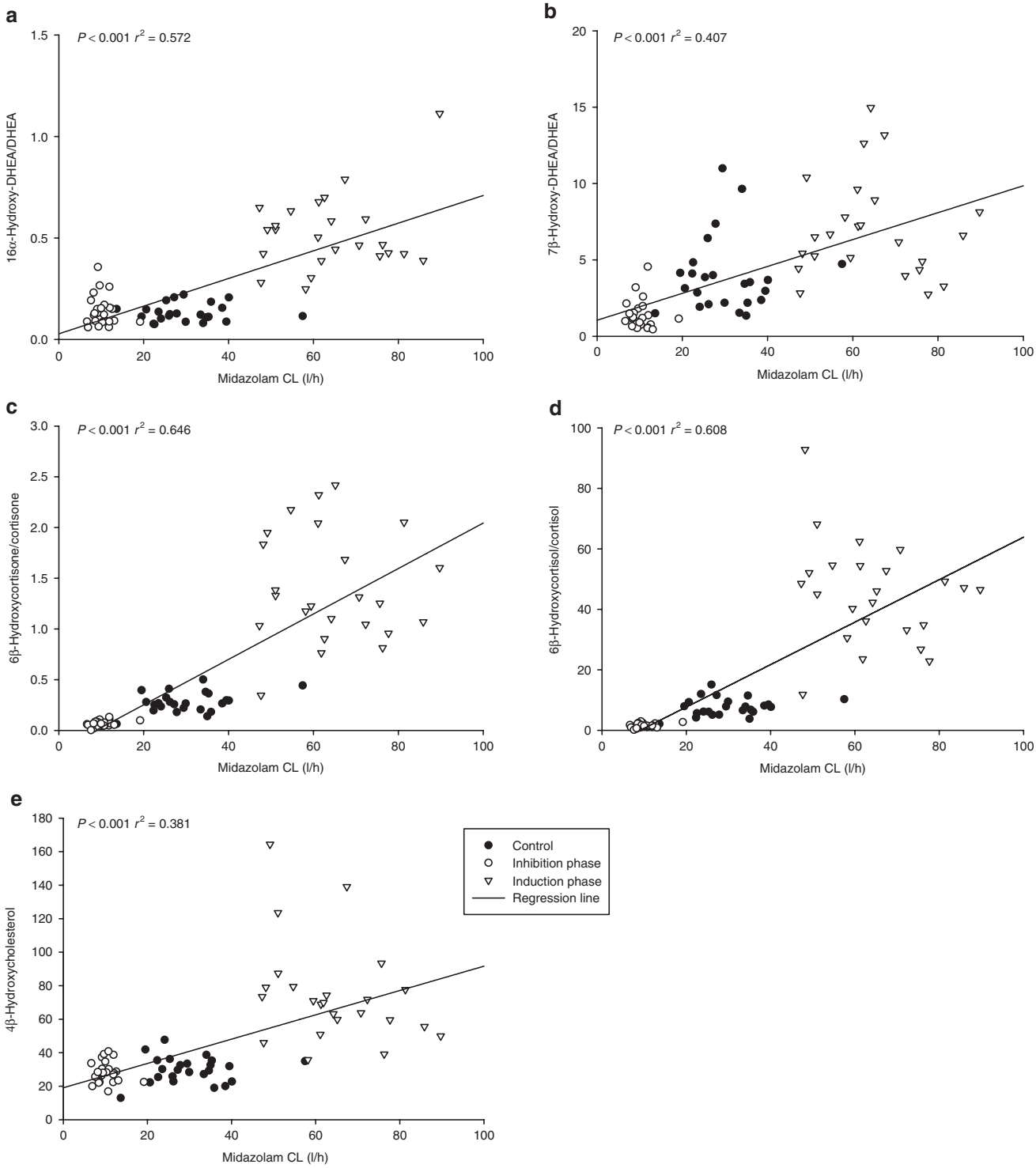


Figure 2 Correlations between midazolam CL and (**a**) 16α-hydroxy-DHEA:DHEA ratio, (**b**) 7β-hydroxy-DHEA:DHEA ratio, (**c**) 6β-hydroxycortisone:cortisone ratio, (**d**) 6β-hydroxycortisol:cortisol ratio, and (**e**) 4β-hydroxycholesterol level (first collection interval). Solid circles, control phase; open circles, CYP3A-inhibited phase; open triangles, CYP3A-induced phase. CL, clearance; CYP, cytochrome P450; DHEA, dehydroepiandrosterone.

to interindividual variability from other factors that were not included as covariates.

DHEA is a cholesterol derivative produced by a series of CYP enzyme– and hydroxysteroid dehydrogenase–dependent reactions.[24] 16α-Hydroxy-DHEA and 7β-hydroxy-DHEA are the major metabolites of DHEA, and CYP3A4 and CYP3A5 are responsible for their production in human liver microsomes.[25] In a previous study, 7β-hydroxy-DHEA was used as a biomarker to compare CYP3A4 and CYP3A7 activities in pediatric and adult human liver microsomes.[26]

Several pharmacometabolomic studies have provided proof of concept for therapeutic drugs. Clayton *et al.*[27] developed a predose predictor for urinary drug metabolites that included values such as the acetaminophen glucuronide:acetaminophen ratio and found an association between predose urinary metabolites and the extent of liver damage in rats. In another study, Clayton *et al.*[28] used predose urinary p-cresol sulfate as a marker of human liver toxicity after acetaminophen administration. Winnike *et al.*[29] suggested that metabolomics could be used to distinguish between acetaminophen responders and nonresponders (thus predicting liver injury) earlier than could changes in alanine aminotransferase. Moreover, pharmacometabolomics can be used to predict metabolic phenotypes for drug-metabolizing enzymes. Although this study produced *CYP3A5*-genotyping results, our goal was to identify phenotypic metabomarkers of CYP3A activity using steroid profiling. Although predicting midazolam CL using a multivariate regression equation with endogenous metabolites results in an unexplained variance of ~30%, the inhibition or induction of CYP3A could be anticipated without probe drug treatment or serial blood sampling for PK analyses. This method may also be useful for predicting interactions between drugs that are metabolized by CYP3A. Furthermore, this approach may provide more accurate predictions of CYP3A inhibition and induction in early-phase clinical trials of new drugs as compared with the less powerful *in vitro* experiments and animal studies currently available.

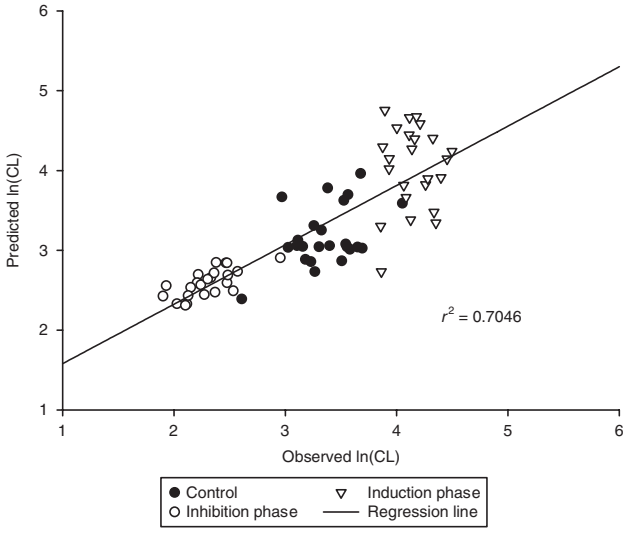


Figure 3 Scatter plot of the predicted midazolam CL values derived from the equation ln(CL) = (2.1539 + 0.2724 × *I* + 0.0101 × DHEA + 0.0910 × *R*1 + 0.6502 × *R*2) vs. the measured midazolam CL values for the 24 subjects (*I* = 1 for *CYP3A5*1/*3* and *I* = 0 for *CYP3A5*3/*3*; *R*1 = 7β-hydroxy-DHEA:DHEA ratio and *R*2 = 6β-hydroxycortisone:cortisone ratio). CL, clearance; DHEA, dehydroepiandrosterone.

Before the study period, we considered the ramifications of different urine collection intervals and subject diets. To identify the optimal urine collection interval for our study design, we evaluated four intervals for each study period. There were no differences among the four urine collection intervals in each treatment phase, suggesting that the timing of urine collection within a given study period is not critical. We assessed the metabolites from a 12-h collection period; however, measurements of the metabolites from spot urine samples from each treatment phase would be helpful for applying our results to other study designs or clinical applications. A controlled diet was necessary for this study because CYP3A inhibition and induction can be influenced by dietary compounds.[30] The same standard diet was provided to all the subjects during the urine collection period of each treatment phase to control for the effects of food on endogenous metabolite levels. Lifestyle factors other than diet can also affect endogenous metabolites; therefore, these factors should be controlled for in metabolomics studies.

The study population was limited to healthy male volunteers. The utility of the selected metabolites should be confirmed in other patient populations, such as elderly subjects or women. For example, women exhibit a 20–50% higher CL of CYP3A-metabolized drugs than do men.[31,32] An exploratory study should be performed to determine whether gender affects metabolic profiles or predictive markers of CYP3A activity. Although only three representative single-nucleotide polymorphisms in each of the *CYP3A4*, *CYP3A5*, and *NR1I2* genes were analyzed here, genetic polymorphisms in CYP3A4/5- and CYP3A-modulating nuclear receptors, such as the constitutive androstane receptor, glucocorticoid receptor, and the estrogen receptor, were not assessed.[33]

In conclusion, we identified endogenous metabolites associated with CYP3A activity in both the inhibited and induced states of the enzyme. We developed an equation to predict midazolam CL based on 7β-hydroxy-DHEA:DHEA ratios, 6β-hydroxycortisone:cortisone ratios, and *CYP3A5* genotypes. Using this equation to predict midazolam CL, CYP3A activity may be anticipated without drug treatment or serial blood sampling for PK analyses. Therefore, a pharmacometabolomics approach can be used to generate predictive markers of CYP3A activity and further insights into variations in CYP-mediated drug metabolism.

METHODS

Subjects. Healthy male volunteers who were aged 20–50 years, weighed over 50 kg, and had body mass indexes of 17–28 kg/m^2 were eligible for participation in the study. The subjects were determined to be healthy based on screening examinations that were performed within 3 weeks before the first administration of the investigational drugs. These examinations included a medical history, physical examination, vital signs, 12-lead electrocardiography, urinary drug screening, serology, and clinical laboratory tests (hematology, chemistry, and urinalysis). Any subjects who had ingested any drugs immediately before the study were excluded. The consumption of grapefruit, grapefruit products, or caffeinated beverages was not permitted from 3 days before the first drug administration until the final day of the study. The study protocol was approved by the institutional review board of Seoul National University Hospital, and it was registered with the US National Institutes of Health

clinical trials database (ClinicalTrials.gov: NCT01215214). The study was conducted at the Clinical Trials Center of Seoul National University Hospital. All the procedures were performed in accordance with the International Conference on Harmonisation of Technical Requirements for Registration of Pharmaceuticals for Human Use–Good Clinical Practice guidelines and the Declaration of Helsinki recommendations for biomedical research involving human subjects. Each subject provided written informed consent before participating in the study.

Chemicals. Reference standards of all steroids examined in this study were obtained from Sigma (St Louis, MO), Steraloids (Newport, RI), or NARL (Pumble, Australia). The internal standards used were as follows: 16,16,17-d_3-testosterone and methyltestosterone for 22 androgens; 2,4,16,16-d_4-estradiol for 18 estrogens; 9,11,12,12-d_4-cortisol for 15 corticoids; 2,2,4,6,6,17α,21,21,21-d_9-progesterone and 2,2,4,6,6,21,21,21-d_8-17α-hydroxyprogesterone for 13 progestins; and 2,2,3,4,4,6-d_6-cholesterol for 2 sterols. All internal standards were purchased from NARL or C/D/N Isotopes (Pointe-Claire, Quebec, Canada). For solid-phase extraction, an Oasis HLB cartridge (3 ml, 60 mg; Waters, Milford, MA) was preconditioned with 3 ml of methanol followed by 3 ml of deionized water. Sodium acetate (reagent grade), acetic acid (glacial, >99.99%), and L-ascorbic acid (reagent grade) were obtained from Sigma. A solution of β-glucuronidase/arylsulfatase from *Helix pomatia* was purchased from Roche Diagnostics (Mannheim, Germany). The trimethylsilylating agent, *N*-methyl-*N*-trifluorotrimethylsilyl acetamide, NH_4I, and dithioerythritol were purchased from Sigma. All organic solvents used were of analytical or high-performance liquid chromatography grade and were purchased from Burdick & Jackson (Muskegon, MI). Deionized water was prepared using a Milli-Q purification system (Millipore, Billerica, MA).

Study design. This was an open-label, fixed-sequence crossover study that was divided into the following three phases: phase I, the control phase, which evaluated the PK of midazolam (i.v., 1 mg); phase II, the CYP3A-inhibited phase, which explored the changes in midazolam (i.v., 1 mg) PK caused by pretreatment with ketoconazole; and phase III, the CYP3A-induced phase, which assessed the effects of rifampicin pretreatment on midazolam (i.v., 2.5 mg) PK (**Figure 4**). For the metabolomic analyses, plasma samples were obtained before each administration of midazolam, and urine samples were collected 24 h before and after each midazolam administration, at 12-h intervals. The subjects were admitted to the study center in the evening 2 days before the administration of the first study drug (day −2). Beginning on the morning of day −1 (9.00 AM), urine samples were collected for 48 h. On day 1, at ~9.00 AM, a single, i.v. dose of 1 mg of midazolam (Bukwang Pharmaceutical, Seoul, Korea) was administered. The subjects were discharged on the morning of day 2. From day 5 through day 7, each subject received 400 mg of ketoconazole (Spike, Choong Wae Pharm, Seoul, Korea) once daily at ~9.00 AM. The subjects were admitted again on the evening of day 7 for the second administration of midazolam. On day 8, the subjects were administered 1 mg of midazolam 1 h after the pretreatment dose of ketoconazole. The blood sampling schedule for the subjects was modified to account for the increased exposure to midazolam, and they were discharged on day 10. On day 13 through day 21, each subject arrived in the morning and received 600 mg of rifampicin (Rifodex, Chong Kun Dang Pharmaceutical, Seoul, Korea) once daily. All the subjects were hospitalized on the evening of day 20 for the third administration of midazolam. On day 22, the subjects were concurrently administered 600 mg of rifampicin and 2.5 mg of midazolam, and the analysis of midazolam PK described for phase I (control) was repeated. During the outpatient period with drug administration, the subjects visited the clinical trials center each morning. The same meals were provided on the urine collection days of all three study phases (days −1 to 1, days 7–8, and days 21–22) to control for the effects of diet on the metabolomic data.

Pharmacogenomic assessments. On day −1, 1-ml blood samples were stored in cryotubes at −70 °C. DNA was extracted from the blood samples using the QIAamp DNA Blood Mini Kit (Qiagen, Hilden, Germany) and was stored at −20 °C. Genotypes were determined using TaqMan Genotyping Assays (Applied Biosystems, Foster City, CA) and a 7500 Real-Time PCR System (Applied Biosystems). A 10-μl PCR reaction mixture was prepared that contained the following components: 5 μl of TaqMan Genotyping Master Mix (Applied Biosystems), 0.5 μl of 20× Drug Metabolism Genotyping Assay Mix (Applied Biosystems), 3.5 μl of DNase-free water, and 1 μl of genomic DNA. Real-time PCR was performed using TaqMan SNP Genotyping Assays (*CYP3A5*3* A6956G, *CYP3A4*18* T878C, and *NR1I2* C-25385T) and a genomic DNA template. The real-time PCR parameters included 50 cycles of holding at 95 °C for 10 min, denaturation at 92 °C for 15 s, annealing at 60 °C for 1 min, and extension at 60 °C for 1 min. The data were analyzed using 7500 Real-Time PCR System Software (version 2.0.1; Applied Biosystems).

PK assessments. To assess the PK of midazolam, 6-ml blood samples were collected during each phase at the following times with respect to the administration of midazolam: before dosing (0 h), and at 10 min, 20 min, 0.5 h, 1 h, 2 h, 3 h, 4 h, 6 h, 8 h, 12 h, 24 h, and 48 h* (*phase II only) after dosing. Plasma was obtained by centrifugation at 2,000*g* at 4 °C for 10 min, and the plasma was immediately stored at −70 °C until use. Following a protein precipitation with acetonitrile, the plasma levels of midazolam, 1′-hydroxymidazolam, and 4-hydroxymidazolam were analyzed with validated liquid chromatography coupled with tandem MS. Midazolam, 1′-hydroxymidazolam, 4-hydroxymidazolam, and flumazenil (as an internal standard) were separated using high-performance liquid chromatography (Agilent 1290 Infinity series; Agilent Technologies, Santa Clara, CA) and were detected with tandem MS (Agilent 6490 Triple Quad; Agilent Technologies) in turbo negative-ion mode and multiple reaction-monitoring mode (m/z = 326.0 > 291.1 for midazolam, 342.1 > 202.8 for 1′-hydroxymidazolam, 342.1 > 325.0

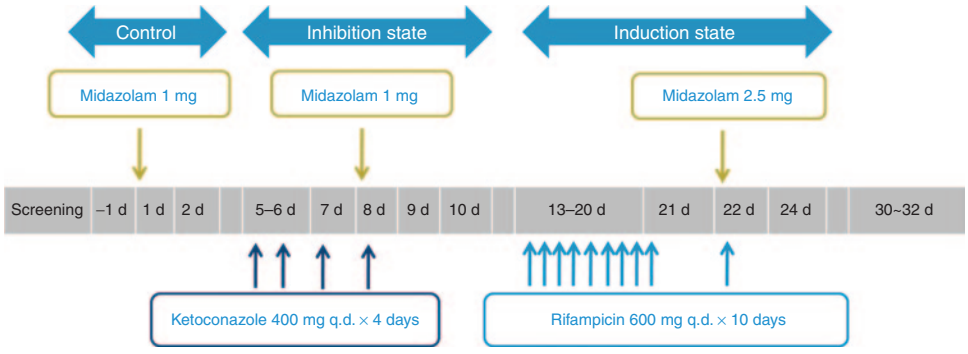


Figure 4 Study schedule and treatment regimens. Midazolam was intravenously administered on days 1, 8, and 22. A 400-mg tablet of ketoconazole was administered on days 5 and 7 and 1 h before midazolam administration on day 8. A 600-mg tablet of rifampicin was administered on days 13–22 (concomitant with midazolam on day 22). d, days.

for 4-hydroxymidazolam, and 304.1 > 258.0 for flumazenil). Briefly, 200 µl of a well-mixed, thawed plasma sample was mixed thoroughly with 50 µl of the internal standard solution (flumazenil). After the addition of 1 ml of methyl tert-butyl ether and 10 min of vortexing, the mixture was centrifuged at 12,000 rpm for 5 min and was frozen at −20 °C for 35 min. The sample was dried in a Speedvac (Thermo Scientific, Rockford, IL) for 90 min at 45 °C and reconstituted with 70% methanol. After the sample was centrifuged at 12,000 rpm for 3 min, the supernatant was injected into the high-performance liquid chromatography–tandem MS system. The lower limits of quantification of midazolam, 1′-hydroxymidazolam, and 4-hydroxymidazolam were 0.1, 0.02, and 0.02 ng/ml, respectively. The standard calibration curves were linear over the range of 0.1–50 ng/ml (coefficients of determination, $r^2 \geq 0.9993$), 0.02–10 ng/ml (coefficients of determination, $r^2 \geq 0.9962$), and 0.02–10 ng/ml (coefficients of determination, $r^2 \geq 0.9990$) for midazolam, 1′-hydroxymidazolam, and 4-hydroxymidazolam, respectively. The intra- and interday accuracy levels ranged from 96.61to 99.61% and from 99.43 to 102.0%, respectively, and the intra- and interbatch precision levels, expressed as the coefficient of variation (%), were <10%. Noncompartmental methods were used to determine the individual PK parameters using Phoenix (version 6.0; Pharsight, Cary, NC). The PK parameters of midazolam included the following: the AUC from time 0 to the last measurable time (AUC_{last}) and from time 0 to infinity (AUC_{inf}, $AUC_{inf} = AUC_{last} + C_{last}/\lambda_z$, where C_{last} is the last measurable concentration and λ_z is terminal slope), the CL (determined as dose/AUC_{inf}), and the terminal half-life. The AUC_{last} values of 1′-hydroxymidazolam and 4-hydroxymidazolam were calculated. The metabolic ratios were calculated as the AUC_{last} of 1′-hydroxymidazolam or as the AUC_{last} of 4-hydroxymidazolam divided by the AUC_{last} of midazolam.

Steroid profiling. The quantitative steroid profiling analyses in urine and plasma were evaluated using previously validated methods.[34,35] Briefly, urine samples (2 ml) spiked with 20 µl of the seven internal standards (d_3-testosterone and d_4-estradiol: 1 µg/ml; d_4-cortisol and d_8-17α-hydroxyprogesterone: 5 µg/ml; and methyltestosterone, d_9-progesterone, and d_6-cholesterol to 10 µg/ml) were extracted with Oasis HLB solid-phase extraction cartridges coupled to a peristaltic pump. After loading a sample onto a cartridge, the cartridge was washed with 2 ml water and eluted twice with 2 ml of methanol. The combined methanol eluates were evaporated under a stream of nitrogen and then 1 ml of 0.2 mol/l acetate buffer (pH 5.2), 100 µl of aqueous 0.2% ascorbic acid, and 50 µl of β-glucuronidase/arylsulfatase were added. After incubation at 55 °C for 3 h, the solution was extracted twice with 2.5 ml of ethyl acetate:*n*-hexane (2:3, vol/vol). Combined organic solvents were evaporated using a N_2 evaporator at 40 °C and further dried in a vacuum desiccator over P_2O_5-KOH for at least 30 min. Finally, the dried residue was derivatized with *N*-methyl-*N*-trifluorotrimethylsilyl acetamide/NH_4I/dithioerythritol (40 µl; 500:4:2, vol/wt/wt) at 60 °C for 20 min, and 2 µl of the resulting mixture was subjected to gas chromatography–MS in selected-ion monitoring mode.

For plasma steroids, the sample (0.4 ml) was diluted with 2.6 ml of acetate buffer (0.2 mol/l, pH 5.2) and subjected to Oasis HLB purification and ethyl acetate:*n*-hexane extraction steps without enzymatic hydrolysis, according to the urinary analysis mentioned above.

Statistical analysis. The statistical analysis was performed with SAS version 9.3 (SAS Korea, Seoul, Korea). The targeted steroids were analyzed using a mixed-effects model with the treatment as the fixed effect and the subject as the random effect on the relative, log-transformed concentrations of the metabolites. The effects of *CYP3A* genotype and urine collection time on the metabolite levels or metabolite ratios were evaluated with a mixed model. The PK parameters were analyzed descriptively and are presented as mean and SD. The effects of ketoconazole or rifampicin pretreatment on the midazolam PK were explored using an analysis of variance model. The analysis of variance model was designed as a mixed model with the treatment as the fixed effect and the subject as the random effect on the following log-transformed PK parameters: AUC_{inf}, CL, and terminal half-life. The administration of midazolam alone served as the reference treatment, and the coadministration of ketoconazole or rifampicin with midazolam was the test treatment. Geometric mean ratios and 90% confidence intervals were calculated for the AUC_{inf} between the test and reference treatments. All the metabolites shown to correlate (with $P < 0.2$) with midazolam CL in the univariate analysis were entered into multivariate linear regression models. The restricted maximum likelihood method was used to analyze the significant covariates of midazolam CL. *CYP3A5* genotype, *NR1I2* genotype, the 6β-hydroxycortisol:cortisol ratio, the 6β-hydroxycortisone:cortisone ratio, the 7β-hydroxy-DHEA:DHEA ratio, and the 16α-hydroxy-DHEA:DHEA ratio were the covariates ultimately evaluated as possible influences on midazolam CL.

SUPPLEMENTARY MATERIAL is linked to the online version of the paper at http://www.nature.com/cpt

ACKNOWLEDGMENTS

This work was supported by a grant from the National Research Foundation of Korea that was funded by the Korean government (MEST) (No. 2010-0009796). We thank Hwa-Suk Kim and Geum-Jwa Ryu for performing the genotyping and the quantification of midazolam and its metabolites. We also acknowledge Sang-Sook Yoon and Hyungmi Ahn for assisting with the clinical trials and performing the statistical analyses, respectively. K.-H.S. received a training program grant from the Korea Healthcare Technology Research and Development Project, Ministry for Health and Welfare of the Republic of Korea (A070001).

AUTHOR CONTRIBUTIONS

J.-Y.C., K.-H.S., M.H.C., K.S.L., K.-S.Y., and I.-J.J. wrote the manuscript; J.-Y.C., K.-H.S., K.-S.Y., and I.-J.J. designed the research; K.S.L. and I.-J.J. analyzed the data; and M.H.C. contributed new reagents/analytical tools.

CONFLICT OF INTEREST

The authors declared no conflict of interest.

Study Highlights

WHAT IS THE CURRENT KNOWLEDGE ON THE TOPIC?

✓ Urinary 6β-hydroxycortisol, 6β-hydroxycortisone, and plasma 4β-hydroxycholesterol are considered to be predictable markers of CYP3A activity.

WHAT QUESTION DID THIS STUDY ADDRESS?

✓ More predictive hepatic CYP3A activity phenotypes could be identified using a pharmacometabolomics approach.

WHAT THIS STUDY ADDS TO OUR KNOWLEDGE

✓ We found that the 16α-hydroxy-DHEA:DHEA and 7β-hydroxy-DHEA:DHEA ratios were highly correlated with hepatic CYP3A activity and that midazolam CL could be predicted using a combination of urinary DHEA levels, 7β-hydroxy-DHEA:DHEA ratios, 6β-hydroxycortisone:cortisone ratios, and *CYP3A5* genotype.

HOW THIS MIGHT CHANGE CLINICAL PHARMACOLOGY AND THERAPEUTICS

✓ The proposed equation for midazolam CL, which includes the 7β-hydroxy-DHEA:DHEA ratio, the 6β-hydroxy-cortisone:cortisone ratio, and the *CYP3A5* genotype, would be helpful for predicting CYP3A-mediated inhibition or induction without the necessity of drug treatment or serial blood sampling for pharmacokinetic analyses.

© 2013 American Society for Clinical Pharmacology and Therapeutics

1. Li, A.P., Kaminski, D.L. & Rasmussen, A. Substrates of human hepatic cytochrome P450 3A4. *Toxicology* **104**, 1–8 (1995).
2. Watkins, P.B. Noninvasive tests of CYP3A enzymes. *Pharmacogenetics* **4**, 171–184 (1994).
3. Rebbeck, T.R., Jaffe, J.M., Walker, A.H., Wein, A.J. & Malkowicz, S.B. Modification of clinical presentation of prostate tumors by a novel genetic variant in CYP3A4. *J. Natl. Cancer Inst*. **90**, 1225–1229 (1998).
4. Lamba, J.K., Lin, Y.S., Schuetz, E.G. & Thummel, K.E. Genetic contribution to variable human CYP3A-mediated metabolism. *Adv. Drug Deliv. Rev*. **54**, 1271–1294 (2002).
5. Kang, Y.S. *et al.* The CYP3A4*18 genotype in the cytochrome P450 3A4 gene, a rapid metabolizer of sex steroids, is associated with low bone mineral density. *Clin. Pharmacol. Ther*. **85**, 312–318 (2009).
6. Elens, L., Bouamar, R., Hesselink, D.A., Haufroid, V., van Gelder, T. & van Schaik, R.H. The new CYP3A4 intron 6 C>T polymorphism (CYP3A4*22) is associated with an increased risk of delayed graft function and worse renal function in cyclosporine-treated kidney transplant patients. *Pharmacogenet. Genomics* **22**, 373–380 (2012).
7. Kukreja, G., Campiani, G., Khurana, J.M., Joshi, B.P. & Grover, S.K. Unexpected formation of hydroxybiphenylmethane derivatives and some new observations on Labat test. *Nat. Prod. Res*. **20**, 1150–1154 (2006).
8. Serruys, P.W. & Kukreja, N. Late stent thrombosis in drug-eluting stents: return of the 'VB syndrome'. *Nat. Clin. Pract. Cardiovasc. Med*. **3**, 637 (2006).
9. Diczfalusy, U. *et al.* 4β-hydroxycholesterol is a new endogenous CYP3A marker: relationship to CYP3A5 genotype, quinine 3-hydroxylation and sex in Koreans, Swedes and Tanzanians. *Pharmacogenet. Genomics* **18**, 201–208 (2008).
10. Lehmann, J.M., McKee, D.D., Watson, M.A., Willson, T.M., Moore, J.T. & Kliewer, S.A. The human orphan nuclear receptor PXR is activated by compounds that regulate CYP3A4 gene expression and cause drug interactions. *J. Clin. Invest*. **102**, 1016–1023 (1998).
11. Schmiedlin-Ren, P., Thummel, K.E., Fisher, J.M., Paine, M.F. & Watkins, P.B. Induction of CYP3A4 by 1 α,25-dihydroxyvitamin D3 is human cell line-specific and is unlikely to involve pregnane X receptor. *Drug Metab. Dispos*. **29**, 1446–1453 (2001).
12. Wang, K., Chen, S., Xie, W. & Wan, Y.J. Retinoids induce cytochrome P450 3A4 through RXR/VDR-mediated pathway. *Biochem. Pharmacol*. **75**, 2204–2213 (2008).
13. Diczfalusy, U., Nylén, H., Elander, P. & Bertilsson, L. 4ß-Hydroxycholesterol, an endogenous marker of CYP3A4/5 activity in humans. *Br. J. Clin. Pharmacol*. **71**, 183–189 (2011).
14. Diczfalusy, U., Kanebratt, K.P., Bredberg, E., Andersson, T.B., Böttiger, Y. & Bertilsson, L. 4β-hydroxycholesterol as an endogenous marker for CYP3A4/5 activity. Stability and half-life of elimination after induction with rifampicin. *Br. J. Clin. Pharmacol*. **67**, 38–43 (2009).
15. Bodin, K. *et al.* Metabolism of 4 β-hydroxycholesterol in humans. *J. Biol. Chem*. **277**, 31534–31540 (2002).
16. Lütjohann, D. *et al.* 4β-hydroxycholesterol as a marker of CYP3A4 inhibition *in vivo* - effects of itraconazole in man. *Int. J. Clin. Pharmacol. Ther*. **47**, 709–715 (2009).
17. Galteau, M.M. & Shamsa, F. Urinary 6β-hydroxycortisol: a validated test for evaluating drug induction or drug inhibition mediated through CYP3A in humans and in animals. *Eur. J. Clin. Pharmacol*. **59**, 713–733 (2003).
18. Aplenc, R. *et al.* CYP3A genotypes and treatment response in paediatric acute lymphoblastic leukaemia. *Br. J. Haematol*. **122**, 240–244 (2003).
19. Cho, J.H., Joo, Y.H., Kim, M.S. & Sun, D.I. Venous hemangioma of parapharyngeal space with calcification. *Clin. Exp. Otorhinolaryngol*. **4**, 207–209 (2011).
20. Corona, G., Rizzolio, F., Giordano, A. & Toffoli, G. Pharmaco-metabolomics: an emerging "omics" tool for the personalization of anticancer treatments and identification of new valuable therapeutic targets. *J. Cell. Physiol*. **227**, 2827–2831 (2012).
21. Phapale, P.B. *et al.* An integrative approach for identifying a metabolic phenotype predictive of individualized pharmacokinetics of tacrolimus. *Clin. Pharmacol. Ther*. **87**, 426–436 (2010).
22. Peng, C.C., Templeton, I., Thummel, K.E., Davis, C., Kunze, K.L. & Isoherranen, N. Evaluation of 6ß-hydroxycortisol, 6ß-hydroxycortisone, and a combination of the two as endogenous probes for inhibition of CYP3A4 *in vivo*. *Clin. Pharmacol. Ther*. **89**, 888–895 (2011).
23. Kanebratt, K.P. *et al.* Cytochrome P450 induction by rifampicin in healthy subjects: determination using the Karolinska cocktail and the endogenous CYP3A4 marker 4β-hydroxycholesterol. *Clin. Pharmacol. Ther*. **84**, 589–594 (2008).
24. Conley, A.J. & Bird, I.M. The role of cytochrome P450 17 α-hydroxylase and 3 β-hydroxysteroid dehydrogenase in the integration of gonadal and adrenal steroidogenesis via the Δ 5 and Δ 4 pathways of steroidogenesis in mammals. *Biol. Reprod*. **56**, 789–799 (1997).
25. Miller, K.K., Cai, J., Ripp, S.L., Pierce, W.M. Jr, Rushmore, T.H. & Prough, R.A. Stereo- and regioselectivity account for the diversity of dehydroepiandrosterone (DHEA) metabolites produced by liver microsomal cytochromes P450. *Drug Metab. Dispos*. **32**, 305–313 (2004).
26. Stevens, J.C. *et al.* Developmental expression of the major human hepatic CYP3A enzymes. *J. Pharmacol. Exp. Ther*. **307**, 573–582 (2003).
27. Clayton, T.A. *et al.* Pharmaco-metabonomic phenotyping and personalized drug treatment. *Nature* **440**, 1073–1077 (2006).
28. Clayton, T.A., Baker, D., Lindon, J.C., Everett, J.R. & Nicholson, J.K. Pharmacometabonomic identification of a significant host-microbiome metabolic interaction affecting human drug metabolism. *Proc. Natl. Acad. Sci. USA* **106**, 14728–14733 (2009).
29. Winnike, J.H., Li, Z., Wright, F.A., Macdonald, J.M., O'Connell, T.M. & Watkins, P.B. Use of pharmaco-metabonomics for early prediction of acetaminophen-induced hepatotoxicity in humans. *Clin. Pharmacol. Ther*. **88**, 45–51 (2010).
30. Stupans, L., Tan, H.W., Kirlich, A., Tuck, K., Hayball, P. & Murray, M. Inhibition of CYP3A-mediated oxidation in human hepatic microsomes by the dietary derived complex phenol, gallic acid. *J. Pharm. Pharmacol*. **54**, 269–275 (2002).
31. Hulst, L.K., Fleishaker, J.C., Peters, G.R., Harry, J.D., Wright, D.M. & Ward, P. Effect of age and gender on tirilazad pharmacokinetics in humans. *Clin. Pharmacol. Ther*. **55**, 378–384 (1994).
32. Kumar, G.N., Walle, U.K. & Walle, T. Cytochrome P450 3A-mediated human liver microsomal taxol 6 alpha-hydroxylation. *J. Pharmacol. Exp. Ther*. **268**, 1160–1165 (1994).
33. Pascussi, J.M., Gerbal-Chaloin, S., Duret, C., Daujat-Chavanieu, M., Vilarem, M.J. & Maurel, P. The tangle of nuclear receptors that controls xenobiotic metabolism and transport: crosstalk and consequences. *Annu. Rev. Pharmacol. Toxicol*. **48**, 1–32 (2008).
34. Moon, J.Y., Jung, H.J., Moon, M.H., Chung, B.C. & Choi, M.H. Heat-map visualization of gas chromatography-mass spectrometry based quantitative signatures on steroid metabolism. *J. Am. Soc. Mass Spectrom*. **20**, 1626–1637 (2009).
35. Ha, Y.W., Moon, J.Y., Jung, H.J., Chung, B.C. & Choi, M.H. Evaluation of plasma enzyme activities using gas chromatography-mass spectrometry based steroid signatures. *J. Chromatogr. B Analyt. Technol. Biomed. Life Sci*. **877**, 4125–4132 (2009).